Characteristics of the PVC rotor R4-10 for the O4 NCal system VIR-0203A-24

Florian Aubin, Eddy Dangelser, Benoit Mours,
Antoine Syx, Pierre Van Hove

IPHC-Strasbourg

February 28, 2024

Contents

1 Introduction **2**

2 Measurement method **2**
2.1 Thermal effects and density . . . 2

3 Raw measurements of the rotor **3**

4 Extracting the geometrical parameters **4**
4.1 Thickness . . . 4
4.2 Radius . . . 5

5 Characterization of the rotor using a simple model **6**
5.1 Theoretical model of the rotor . . . 6
5.2 Thickness . . . 6
5.3 Radius . . . 6
5.4 Expected NCal signal and uncertainties . . . 6

6 Characterization of the rotor using an advanced model **7**
6.1 Thickness . . . 7
6.2 Radius . . . 7
6.3 Counterweights . . . 8
6.4 Opening angles and asymmetry . . . 9
6.5 Expected NCal signals and uncertainties . . . 9
6.5.1 Advanced geometry including chamfers and counterweight . . . 9
6.5.2 Remaining geometry uncertainty . . . 10
6.5.3 Uncertainties . . . 10

A Appendix **12**

1 Introduction

Since the aluminum rotors produce a small magnetic field at twice the rotation frequency we investigate the possibility of using polyvinyl chloride (PVC) as the material for the O4 rotors. It is expected that PVC rotors will produce a reduced magnetic field when operating.

This note discusses the metrology of a rotor machined at IPHC from the first set of PVC material and follows a similar discussion made on the aluminum rotors R4-01 in VIR-0591C-22 and R4-05 in VIR-0859A-22. The drawings and figures of the PVC rotor can be found at the end of this technical note. The rotor has been engraved IPHC-R4-10 on one side and painted on the other side.

2 Measurement method

To determine the geometry of the rotor we will use the same method as for R4-01 (see VIR-0591C-22). The thickness was measured using 16*2 = 32 points for the sectors and 8*2 = 16 points for the inner part. In addition we measured the outer diameter using four more points than the previous rotors for a total of 4*3 = 12 points. The measurement points are shown in fig. 1. We will use the drawing values for the inner diameter.

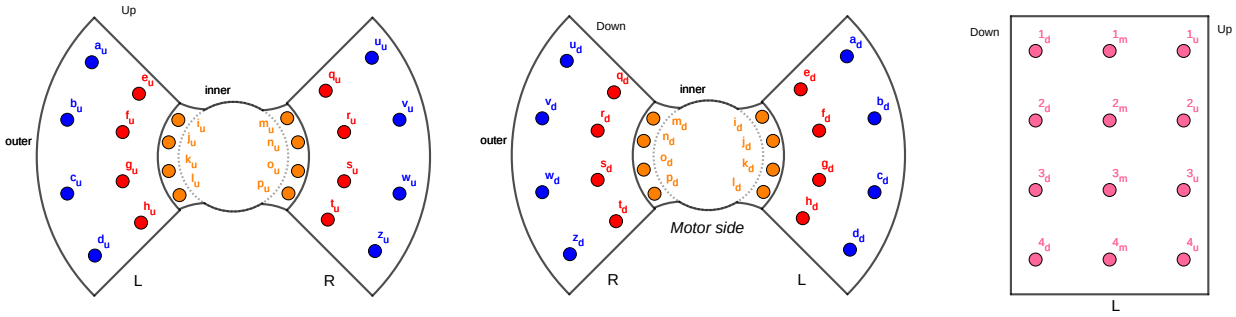

Figure 1: Outline of the faces of the rotor with the measurement points. Left is face up, center is face down and right is the side view of the left sector. Sectors have been labelled L for left sector and R for right sector.

The tool used to measure the thickness and the outer diameter is a measuring column "Garant 44 5350_600 HC1" (see VIR-0160A-22) with a given precision of 1.8+L/600 μm (L the measured length in mm). Steel reference blocks of 100.000 mm and 90.000 mm (see certificate of inspection provided at the end of this note) were used to check the accuracy of the measuring column, the standard deviation from the nominal values is of the order of the uncertainty of the measuring column (2 μm).

The measuring column was operated on a metrology table with a value ranging from 0 to 2 μm. The rms of the 16 values is 0.9 μm.

We measured the opening angles of the sectors using a video measuring microscope "Garant MM2" (see VIR-0591C-22) with a given precision of 2.9+L/100 μm at 95% CL (L the measured length in mm).

2.1 Thermal effects and density

As discussed in VIR-0193A-24, the thermal effects on the PVC must be taken into account (80 μm/m/°C). As for the previous rotors the results will be expressed at a reference temperature of 23°C.

The temperature inside the NE building might fluctuate around $T_{\text{build}} = 21.5$°C. The temperature of the motor can increase by up to several tens of degrees depending on the rotation speed. This will increase the

rotor temperature. We expect to operate the rotors continuously at around 20 Hz, the aluminum rotors have been operating since summer 2023 at this frequency and the temperature of the box is seen to be constant at around 23°C with no more than 1.5°C of maximum deviation. The same temperature has been observed with the PVC rotors which were installed on February 20, 2024. The gravitational strain h is therefore computed assuming a reference temperature $T_{\text{ref}} = 23 \pm 1.5$°C.

The uncertainty on the strain h is the following:

$$\begin{aligned} h &\propto \rho_{rot}\, b\, r_{max}^4 \\ &\propto \frac{m\, r_{max}^2}{\pi} \end{aligned} \tag{1}$$

Using $r(T) = r(1 + \alpha_T)$ (with the temperature factor $\alpha_T = C_T(T_{\text{build}} - T_{\text{ref}})$) we have:

$$\begin{aligned} h(T) &\propto r_{max}^2(T) \\ &\propto r_{max}^2(1 + \alpha_T)^2 \end{aligned} \tag{2}$$

We compute the relative uncertainty of h on the temperature T:

$$\left|\frac{\partial h}{\partial T}\right| \frac{\Delta T}{h} = \frac{2C_T}{1 + C_T(T_{\text{build}} - T_{\text{ref}})} \Delta T \tag{3}$$

3 Raw measurements of the rotor

This section presents the raw measurements made on the rotor at the ambient temperature of 21.2°C for the thickness and 21.7°C for the diameter. Table 1 shows the thickness measurements according to the measurement points defined in fig. 1. The rotor is laying on the table. The rotor surface as well as the table are not perfectly flat. Some space could be present in between that should be substracted when computing the rotor thickness as discussed later.

Measurement point	L sector		Measurement point	R sector	
	Up	Down		Up	Down
a	104.394	104.398	q	104.407	104.409
b	104.397	104.397	r	104.405	104.408
c	104.399	104.398	s	104.406	104.409
d	104.394	104.400	t	104.407	104.409
e	104.407	104.409	u	104.393	104.399
f	104.406	104.407	v	104.392	104.401
g	104.407	104.408	w	104.393	104.402
h	104.407	104.409	z	104.397	104.404
i	101.569	101.385	m	101.567	101.385
j	101.569	101.384	n	101.565	101.386
k	101.566	101.384	o	101.563	101.383
l	101.566	101.384	p	101.562	101.383

Table 1: Raw measurements of the height in mm for each point at 21.2°C on L and R sectors of R4-10.

Table 2 displays the diameter measurements. The measurements were made on 4*3 diameters (three parts of each diameter, the up, middle and down sides of the rotor).

Measurement point	Up	Middle	Down
1	207.655	207.656	207.655
2	207.656	207.655	207.655
3	207.656	207.656	207.656
4	207.658	207.656	207.656

Table 2: Raw measurements of the diameter in mm for each point at 21.7°C on R4-10.

Theoretical values were taken for the inner radius r_{min} = 29 mm and the radius for the counterweight $r_{\text{counterweight}}$ = 40 mm (see drawing at the end of this note).

4 Extracting the geometrical parameters

4.1 Thickness

We need to correct the possible gap between the rotor and the measuring table. Assuming that the table is flatter than the rotor surface we can extract the gap from the measurement of the top surface considering the plane tangents to the highest points (asking them to be on both sectors). For this rotor these points are e, h, t for the up and e, h, t for the down face (see fig. 1). Using the measurements in table 1 we can compute a plane equation for each side of the rotor in cartesian coordinates:

$$\text{Up plane equation} : z = 104.407 \tag{4}$$

$$\text{Down plane equation} : z = 104.409 \tag{5}$$

Using eqs. (4) and (5) the gap can be determined, see table 3. The maximum rms of the gap for a sector is 15 μm.

Measurement point	L sector		Measurement point	R sector	
	Up	Down		Up	Down
a	13	11	q	0	0
b	10	12	r	2	1
c	8	11	s	1	0
d	13	9	t	0	0
e	0	0	u	14	10
f	1	2	v	15	8
g	0	1	w	14	7
h	0	0	z	10	5

Table 3: Gap computed in μm on up and down sides of both sectors of R4-10.

We can then compute the rotor thickness for each point by removing these gaps. If one of the raw values is lower than the corrected thickness we take this lowest value. The thickness of the inner part is computed by taking into account the air between the closest measurement point on the sector and the measurement point on this part, the average value between up and down is taken as our final value. The value of each point is shown in table 4 at 23°C.

Measurement point	L sector	Measurement point	R sector
a	104.409	q	104.422
b	104.412	r	104.420
c	104.413	s	104.421
d	104.409	t	104.422
e	104.422	u	104.408
f	104.421	v	104.407
g	104.422	w	104.408
h	104.422	z	104.412
i	98.560	m	98.558
j	98.531	n	98.559
k	98.557	o	98.553
l	98.556	p	98.551

Table 4: Measurements of the thickness in mm for each point at 23°C on L and R sectors of R4-10.

4.2 Radius

Using comparators while the rotor is rotating on its axis we can determine the deformation on both sectors and compute different radii values. Table 5 shows the raw measurements using comparators on L and R sectors. The measurements were made on the up, middle and down sides of L and R sectors using three comparators for a total of 5*3*2=30 points (the first and last points are near the edge of the sectors).

Measurement point	L sector			R sector		
	Up	Middle	Down	Up	Middle	Down
A	10	2	0	0	-2	0
B	5	2	0	0	-2	0
C	0	0	0	0	-2	-5
D	0	0	0	7	-2	-5
E	0	0	0	5	-2	-10

Table 5: Raw measurements in μm of the comparators for the L and R sectors of R4-10.

The zeroing of the comparators was made arbitrarily close to the edge of the sector. The offsets shown in table 5 are measured relative to this reference.

To compute the radius per measurement point we use the following process: First we compute the mean deformation for one comparator. Then we remove this mean deformation to each measurement of this comparator. The corrected shift value is added to the mean of the associated up, middle or down diameter computed using table 2 at 21.7°C. This process is repeated for each comparator. The final radius for each point are shown in table 6.

Measurement point	L sector			R sector		
	Up	Center	Down	Up	Center	Down
A	103.835	103.830	103.830	103.825	103.826	103.830
B	103.830	103.830	103.830	103.825	103.826	103.830
C	103.825	103.828	103.830	103.825	103.826	103.825
D	103.825	103.828	103.830	103.832	103.826	103.825
E	103.825	103.828	103.830	103.830	103.826	103.820

Table 6: Radius measurements in mm at 21.7°C for the L and R sectors of R4-10.

5 Characterization of the rotor using a simple model

5.1 Theoretical model of the rotor

Using the analytical strain equation at 2f shown in eq. (6) with the rotor design parameters at a distance of 1.7 m, an angle to beam axis of $34.7°$ and a twist angle of $12°$ we compute a value of $1.1480 \times 10^{-18}/(2f_{rot})^2$.

$$h_{2f}(\psi) = \frac{G\rho_{rot}\ b\ sin(\alpha)(r_{max}^4 - r_{min}^4)}{32L\pi^2 f_{2rot}^2}\ (9\cos^2\psi\cos\phi + 6\cos\psi\sin\psi\sin\phi) \tag{6}$$

When using FROMAGE v1r2 with the same parameters we obtain $1.1415 \times 10^{-18}/(2f_{rot})^2$. The 0.569% between both results is due to the mirror and rotor finite element geometry computed in FROMAGE.

At 2.1 m the difference between the analytical formula and FROMAGE is 0.373% as it converges to the point mass approximation when the distance increases.

5.2 Thickness

A simple model can be used to determine a mean value for the thickness and its uncertainty.

As shown on fig. 1, a total of $16 + 8 = 24$ points were used to compute the thickness of each sector.

For the simple model we take the thickness as the mean value of table 4: 104.416 mm at 23°C. Since we have a limited number of measurement points, to be conservative we take the thickness uncertainty as the rms of table 4 (6.3 μm) to which we add linearly the metrology table uncertainty (0.9 μm) and the tool uncertainty (2.0 μm). Therefore, for this simple model, the thickness is 104.416 $\pm$ 0.009 mm.

5.3 Radius

For the simple model we take the radius as the mean value of table 6: 103.839 mm at 23°C. Using a linear sum of the rms of table 6 (3 μm) and the tool uncertainty (2.2 μm) we take an uncertainty of 5 μm on the mean radius.

5.4 Expected NCal signal and uncertainties

The geometry previously used to describe the rotors as a simple model is represented in fig. 2a. We chose to take into account the housing space for the counterweights on each side of the rotor as seen in the drawing at the end of the note, each space is 3 mm thick and 40 mm of radius wide. The new simple model geometry used for this rotor is then represented in fig. 2b.

Using FROMAGE on the previous 2a geometry we compute the following 2f strain on the mirror at a distance of 1.7 m, an angle to beam axis of $34.7°$ and a twist angle of $12°$:

- strain(2f) $= \dfrac{1.1346 \times 10^{-18}}{(2f_{rot})^2}$

Using FROMAGE on the new 2b geometry we compute the following 2f strain on the mirror at a distance of 1.7 m, an angle to beam axis of $34.7°$ and a twist angle of $12°$:

- strain(2f) $= \dfrac{1.1336 \times 10^{-18}}{(2f_{rot})^2}$

This last value will be compared to the advanced model. We point out that the relative difference between both simple models is 0.088%.

The uncertainties considered for this model are displayed in table 7.

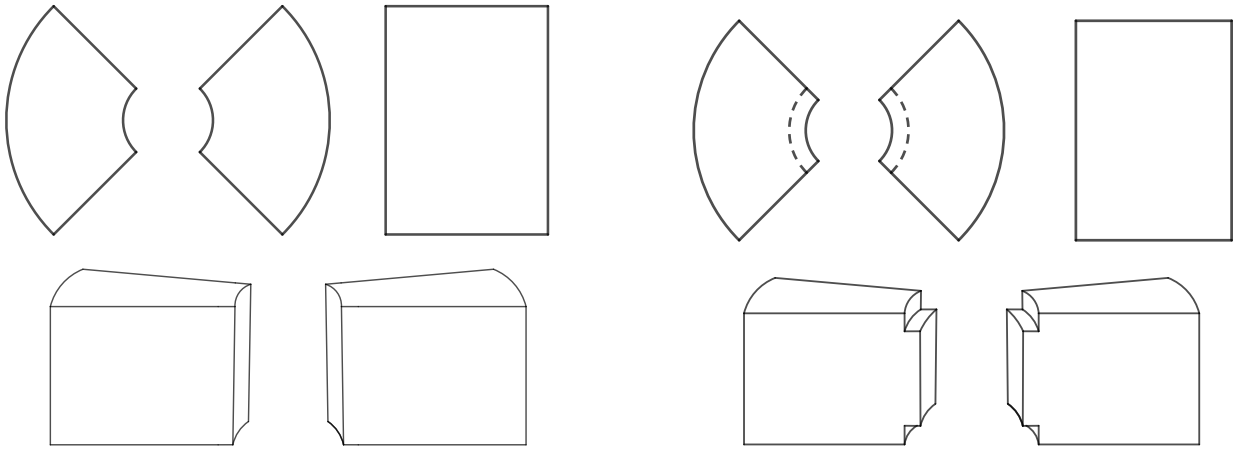

(a) Previous simple model geometry model with uniform sectors.

(b) New simple model geometry including the counterweight spacings.

Figure 2: (a) is the previously used simple geometry, (b) is the new version used for the PVC rotor. For each figure, left top is a top view, right top is a side view (external sector) and bottom is a tilted view of the rotor.

R4-10 rotor parameter simple model (23°C)			NCal 2f signal uncertainty	
name	value	uncertainty	formula	value (%)
Density ρ (kg.m^{-3})	1442.3	0.2	$\delta\rho/\rho$	0.014
Thickness b (mm)	104.416	9×10^{-3}	$\delta b/b$	0.009
r_{max} (mm)	103.839	5×10^{-3}	$4\delta r_{max}/r_{max}$	0.020
G (m^3.kg^{-1}.s^{-2})	$6.674\,30 \times 10^{-11}$	1.5×10^{-15}	$\delta G/G$	0.002
Temperature T (°C)	23	1.5	$\left\lvert\frac{\partial h}{\partial T}\right\rvert \frac{\Delta T}{h}$	0.024
Quadratic sum				0.035

Table 7: Uncertainties on the amplitude of the calibration signal at 2f from the R4-10 rotor simple model geometry..

6 Characterization of the rotor using an advanced model

6.1 Thickness

A more advanced model can be used considering the deformations on the surfaces of the sectors for better accuracy. Each measurement point of table 4 can be considered as a sub-sector with its own thickness.

The uncertainty on this value is more complex to evaluate. As a conservative approach we use the maximum rms of the deviation to a plane for each sector (6 μm see section 4.1) to which we add linearly the uncertainty on the flatness of the measurement table (0.9 μm) as well as the measurement tool (2.0 μm). The total uncertainty on the thickness is 9 μm.

6.2 Radius

On fig. 1 we divided the external sectors in 4 sub-sectors for each sector (blue points). We convert the point of table 6 to the grid of fig. 1 by averaging the two closest values and converting them to 23°C. The results are shown in table 8. We notice that the L sector is on average 2 μm larger than the R sector.

Radius	L sector			R sector		
	Up	Center	Down	Up	Center	Down
1	103.844	103.841	103.841	103.836	103.837	103.841
2	103.839	103.840	103.841	103.836	103.837	103.838
3	103.836	103.839	103.841	103.840	103.837	103.836
4	103.836	103.839	103.841	103.842	103.837	103.833

Table 8: Radius measurements (in mm at 23°C) for the L and R sectors of R4-10.

The maximum rms of the radii for each sector is 2.5 μm. The tool uncertainty is 2.2 μm. Like for the thickness we use a linear sum and find the uncertainty on both radii to be 5 μm.

6.3 Counterweights

A pair of counterweights have been designed to reduce the unbalance of the rotor using the same method as R4-06 in section 6.3 of VIR-0860B-22. The mass deduced from this method was then divided into 2 counterweights placed on each side of the rotor to reduce the lateral unbalance of the rotor due to the previous use of a single counterweight. These counterweights are made of PVC ($\rho_{\text{PVC}} = 1442.3$ kg.m^{-3}) a picture showing their initial geometry is shown fig. 3. the disk on the left was designed so the motor would fit in its center, the disk on the right fits the axle of the rotor. The thickness of the disks is 3 mm, with an outer radius measuring 40 mm. On the motor side, the inner radius of the disk is 21.75 mm, while on the axle side, it measures 10 mm.

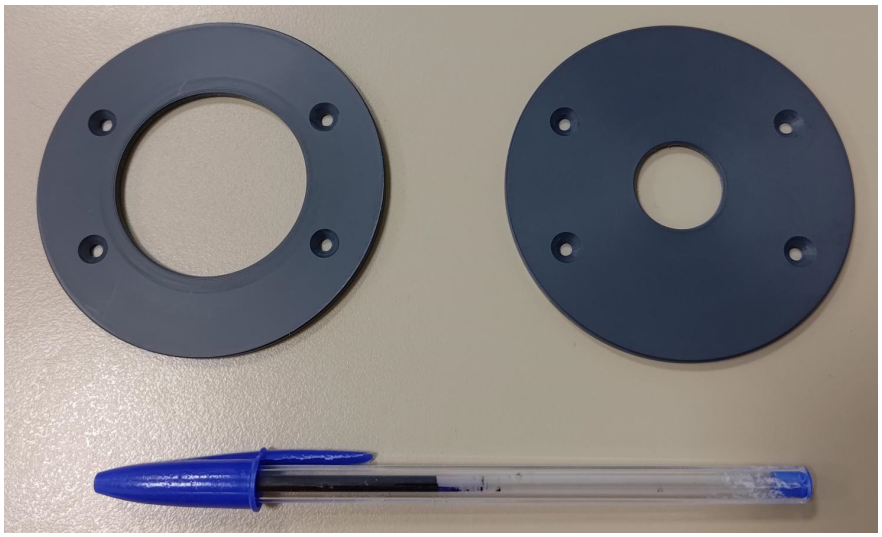

Figure 3: Picture of the PVC disks used as counterweights for the PVC rotor.

Figure 4 shows the geometry of the machined counterweights to balance the rotor with a material cut following a chord of 55.8 mm (see black areas on fig. 4).

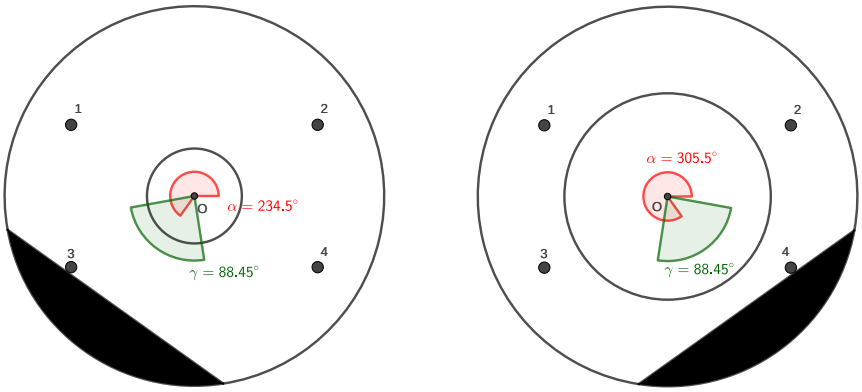

Figure 4: Outline of the counterweights for R4-10. The black areas represents the material removed.

6.4 Opening angles and asymmetry

The opening angles of the full and empty sectors have been measured using a video microscope with the same method as for R4-01.

The measurements are shown in table 9. The center value corresponds to the mean of up and down measurements.

Opening angle	Up	Center	Down
L	1.57107	1.57046	1.56985
R	1.57101	1.57047	1.56993
L-R	1.57089	1.57195	1.57300
R-L	1.57022	1.57031	1.57040

Table 9: Opening angle measurements in rad for the L, R full sectors and L-R, R-L empty sectors of R4-10.

These measurements allow us to compute the signal with different opening angles and an asymmetry between the sectors. These measured opening angles will be included in the advanced model described in the next section.

Using FROMAGE on the advanced rotor geometry we can compare the effects of the opening angles between perfectly symmetrical sectors and the values of table 9. This gives a relative difference below 0.001% on the rotor signal at 2f.

The uncertainty on α = 0.2 mrad is the same as for R4-01, we use FROMAGE to propagate it on the measurements shown in table 9 and find a relative deviation of 0.002% on the rotor signal at 2f. This value will be taken as the opening angle and asymmetry uncertainty.

6.5 Expected NCal signals and uncertainties

6.5.1 Advanced geometry including chamfers and counterweight

The geometry used to describe the rotor as an advanced model is represented in fig. 5. The external parts of the sectors are divided in 3 sub-sectors each to correspond to the different radii determined. In addition we include the counterweight, the opening angles and asymmetry of the sectors. The screws and screw holes are not taken into account since they are placed symmetrical they should not impact the 2f signal.

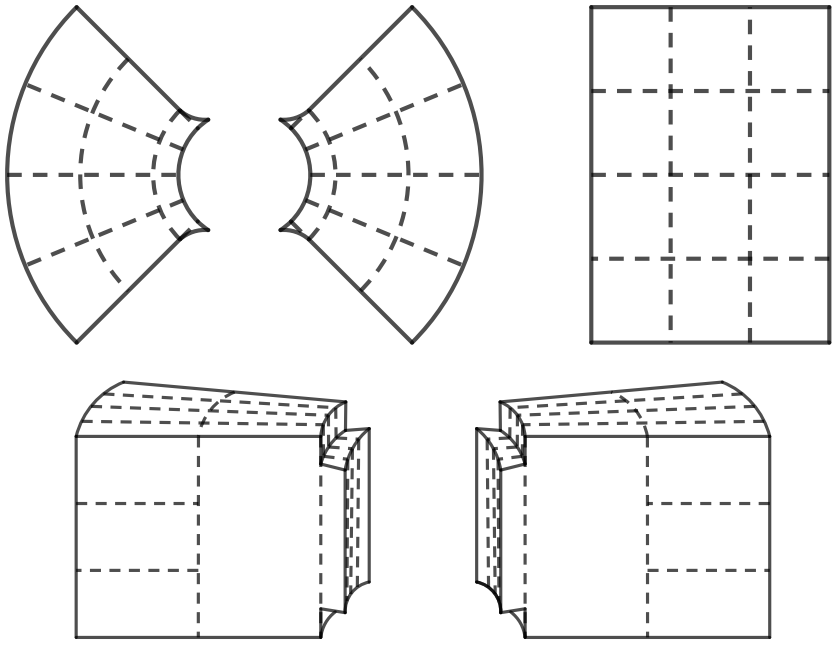

Figure 5: Advanced model geometry used to describe the rotor. Top left is a front view, top right is a side view (external sub-sectors) and bottom is a tilted view of the sectors. Only the 4 external part sectors are divided in 3 sub-sectors each. The chamfers are visible on the inner radius.

Using FROMAGE at a distance of 1.7 m, an angle of $34.7°$ and a twist of $12°$ on this geometry gives the following strains:

- strain(1f) $= \dfrac{1.5664 \times 10^{-20}}{(1 f_{rot})^2}$
- strain(2f) $= \dfrac{1.1336 \times 10^{-18}}{(2 f_{rot})^2}$

The relative deviation to the simple model at 2f is just below 0.001%.

6.5.2 Remaining geometry uncertainty

Other geometrical defects are probed by the remaining 1f signal computed with the advanced geometry as described for the rotor R4-01 (see section 7.5.4 of VIR-0591C-22). For this rotor the 1f signal is 5 times smaller than for R4-01. Nevertheless we will use the $5 \times 10^{-4}\%$ R4-01 remaining geometry uncertainty as a conservative approach.

6.5.3 Uncertainties

To set an uncertainty on the strain(2f) from the description of the geometry we take the difference between the simple model (strain(2f) $= 1.1336 \times 10^{-18}/(2f)^2$) and the advanced model (strain(2f) $= 1.1336 \times 10^{-18}/(2f)^2$). This deviation, below 0.001%, is reported in table 10 as modelling uncertainty.

The uncertainties considered for this full model are displayed in table 10. We point out that the elongation of the material caused by the rotation is not taken into account in this technical note.

R4-10 rotor parameter advanced model (23°C)			NCal 2f signal uncertainty	
name	mean value	uncertainty	formula	value (%)
Density ρ (kg.m^{-3})	1442.3	0.2	$\delta\rho/\rho$	0.014
Thickness b left sector (12 sub-sectors) (mm) Thickness b right sector (12 sub-sectors) (mm)	104.416 104.415	9×10^{-3}	$\delta b/b$	0.008
r_{max} left sector (12 ext sub-sectors) (mm) r_{max} right sector (12 ext sub-sectors) (mm)	103.840 103.838	5×10^{-3}	$4\delta r_{max}/r_{max}$	0.018
G (m^3.kg^{-1}.s^{-2})	$6.674\,30 \times 10^{-11}$	1.5×10^{-15}	$\delta G/G$	0.002
Temperature T (°C)	23	1.5	$\left\lvert\frac{\partial h}{\partial T}\right\rvert \frac{\Delta T}{h}$	0.024
Modelling Uncertainty				0.001
FROMAGE grid uncertainty				0.005
Opening angle and sector asymmetry uncertainty				0.002
Remaining geometry uncertainty				$<5 \times 10^{-4}$
Total uncertainty from the rotor (quadratic sum)				0.034

Table 10: Uncertainties on the amplitude of the calibration signal at 2f from the R4-10 rotor advanced model geometry at 23°C.

A Appendix

```
### This is a cfg file for a more realistic geometry of the mirror and the Virgo NCal R4-10 (2024)

### ALL THE OBJECTS ARE DEFINED IN THE MIRROR'S FRAME (O,x,y,z),
### with O the center of the mirror, x axis along the ITF's beam toward the beam-splitter,
### y axis orthogonal to x in the plane of the ITF,
### z axis orthogonal to the plane of the ITF upward

### MIRROR DEFINITION

GRID_SIZE 12 30 8

CYLINDER 2202. 0 0.175 0.2 360 0 0 0

GRID_SIZE 1 1 1

# Defining the flats on the edge of the mirror
CUT_CYL 2202. 0.175 0.2 0.05 0 0
CUT_CYL 2202. 0.175 0.2 0.05 0 180

# Defining the ears and anchors of the mirror
CUBOID 2202. 0.090 0.010 0.015  0     0.1782 -0.0125
CUBOID 2202. 0.090 0.010 0.015  0    -0.1782 -0.0125
CUBOID 2202. 0.039 0.008 0.008 -0.02 -0.1772 -0.024
CUBOID 2202. 0.039 0.008 0.008 -0.02  0.1772 -0.024
CUBOID 2202. 0.039 0.008 0.008  0.02 -0.1772 -0.024
CUBOID 2202. 0.039 0.008 0.008  0.02  0.1772 -0.024

### ROTOR DEFINITION: CYLINDER DENSITY INNER_RADIUS OUTER_RADIUS THICKNESS OPEN_ANGLE r z theta

ROTOR_CYLINDRICAL 1.7 34.7 0 0 12

### COUNTERWEIGHT AXLE
GRID_SIZE 8 17 14
CYLINDER 1442.3 0.010 0.040 0.003 360 0 0.050780345348 0
GRID_SIZE 1 1 1
CUT_CYL 1442.3 0.040 0.003 0.0558 0.050780345348 234.5

### COUNTERWEIGHT MOTOR
GRID_SIZE 8 17 14
CYLINDER 1442.3 0.02175 0.040 0.003 360 0 -0.050780345348 0
GRID_SIZE 1 1 1
CUT_CYL 1442.3 0.040 0.003 0.0558 -0.050780345348 234.5

# TRES RAPIDE
#GRID_SIZE 4 4 4
# RAPIDE
GRID_SIZE 8 17 14
# LENT
#GRID_SIZE 8 65 40

### L sector

## Inner part
OUTER_FILLET 1442.3 0.029 0.098560 0 0.01 -11.2476 146.2573
```

```
CYLINDER 1442.3 0.029 0.04 0.098560 22.4951 0 0 146.2573
CYLINDER 1442.3 0.029 0.04 0.098561 22.4951 0 0 168.7524
CYLINDER 1442.3 0.029 0.04 0.098557 22.4951 0 0 191.2476
CYLINDER 1442.3 0.029 0.04 0.098556 22.4951 0 0 213.7427
OUTER_FILLET 1442.3 0.029 0.098556 0 0.01 11.2476 213.7427

## Middle part
CYLINDER 1442.3 0.04 0.072 0.104422 22.4951 0 0 146.2573
CYLINDER 1442.3 0.04 0.072 0.104421 22.4951 0 0 168.7524
CYLINDER 1442.3 0.04 0.072 0.104422 22.4951 0 0 191.2476
CYLINDER 1442.3 0.04 0.072 0.104422 22.4951 0 0 213.7427

## Outer part
CYLINDER 1442.3 0.072 0.103844 0.034803010912 22.5039 0 0.034803010912 146.2442
CYLINDER 1442.3 0.072 0.103841 0.034803010912 22.4951 0 0 146.2573
CYLINDER 1442.3 0.072 0.103841 0.034803010912 22.4864 0 -0.034803010912 146.2704

CYLINDER 1442.3 0.072 0.103839 0.034804011056 22.5039 0 0.034804011056 168.7481
CYLINDER 1442.3 0.072 0.103840 0.034804011056 22.4951 0 0 168.7524
CYLINDER 1442.3 0.072 0.103841 0.034804011056 22.4864 0 -0.034804011056 168.7568

CYLINDER 1442.3 0.072 0.103836 0.034804344437 22.5039 0 0.034804344437 191.2519
CYLINDER 1442.3 0.072 0.103839 0.034804344437 22.4951 0 0 191.2476
CYLINDER 1442.3 0.072 0.103841 0.034804344437 22.4864 0 -0.034804344437 191.2432

CYLINDER 1442.3 0.072 0.103836 0.034803010912 22.5039 0 0.034803010912 213.7558
CYLINDER 1442.3 0.072 0.103839 0.034803010912 22.4951 0 0 213.7427
CYLINDER 1442.3 0.072 0.103841 0.034803010912 22.4864 0 -0.034803010912 213.7296

### R sector

## Inner part
OUTER_FILLET 1442.3 0.029 0.098558 0 0.01 11.2478 33.6963
CYLINDER 1442.3 0.029 0.04 0.098558 22.4957 0 0 33.6963
CYLINDER 1442.3 0.029 0.04 0.098559 22.4957 0 0 11.2010
CYLINDER 1442.3 0.029 0.04 0.098553 22.4957 0 0 348.7057
CYLINDER 1442.3 0.029 0.04 0.098551 22.4957 0 0 326.2104
OUTER_FILLET 1442.3 0.029 0.098551 0 0.01 -11.2478 326.2104

## Middle part
CYLINDER 1442.3 0.04 0.072 0.104422 22.4957 0 0 33.6963
CYLINDER 1442.3 0.04 0.072 0.104420 22.4957 0 0 11.2010
CYLINDER 1442.3 0.04 0.072 0.104421 22.4957 0 0 348.7057
CYLINDER 1442.3 0.04 0.072 0.104422 22.4957 0 0 326.2104

## Outer part
CYLINDER 1442.3 0.072 0.103836 0.0348026775307 22.5050 0 0.0348026775307 33.7078
CYLINDER 1442.3 0.072 0.103837 0.0348026775307 22.4957 0 0 33.6963
CYLINDER 1442.3 0.072 0.103841 0.0348026775307 22.4876 0 -0.0348026775307 33.6847

CYLINDER 1442.3 0.072 0.103836 0.0348023441493 22.5050 0 0.0348023441493 11.2048
CYLINDER 1442.3 0.072 0.103837 0.0348023441493 22.4957 0 0 11.2010
CYLINDER 1442.3 0.072 0.103838 0.0348023441493 22.4876 0 -0.0348023441493 11.1971

CYLINDER 1442.3 0.072 0.103840 0.0348026775307 22.5050 0 0.0348026775307 348.7018
CYLINDER 1442.3 0.072 0.103837 0.0348026775307 22.4957 0 0 348.7057
```

```
CYLINDER 1442.3 0.072 0.103836 0.0348026775307 22.4876 0 -0.0348026775307 348.7096

CYLINDER 1442.3 0.072 0.103842 0.034804011056 22.5050 0 0.034804011056 326.1989
CYLINDER 1442.3 0.072 0.103837 0.034804011056 22.4957 0 0 326.2104
CYLINDER 1442.3 0.072 0.103833 0.034804011056 22.4876 0 -0.034804011056 326.2220

### GENERAL PARAMETERS

STEP 22.5 16

ARM_LENGTH 3000

SIGNAL 2
```

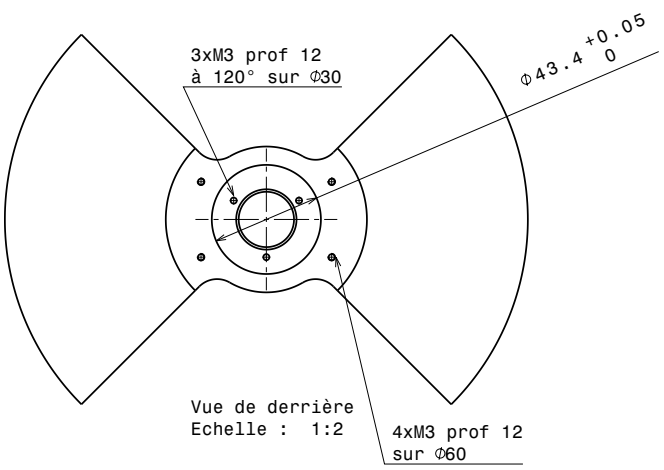

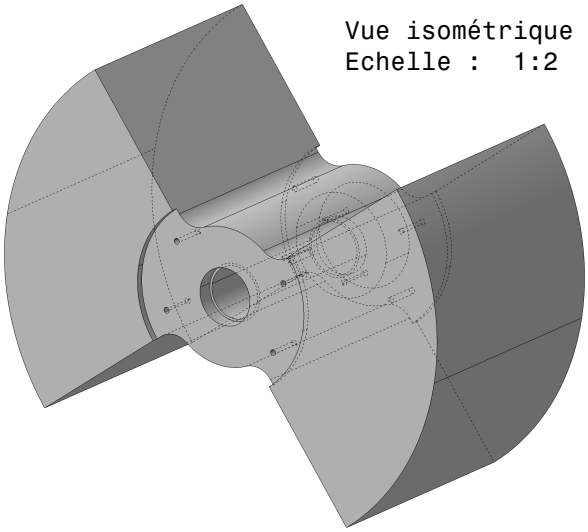

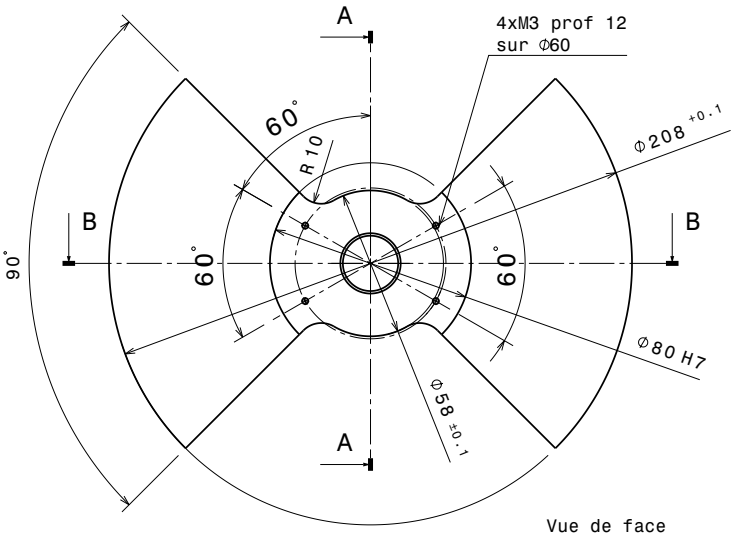

Vue de face
Echelle : 1:2

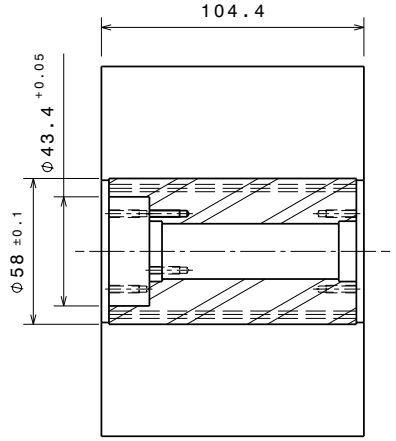

Coupe A-A
Echelle : 1:2

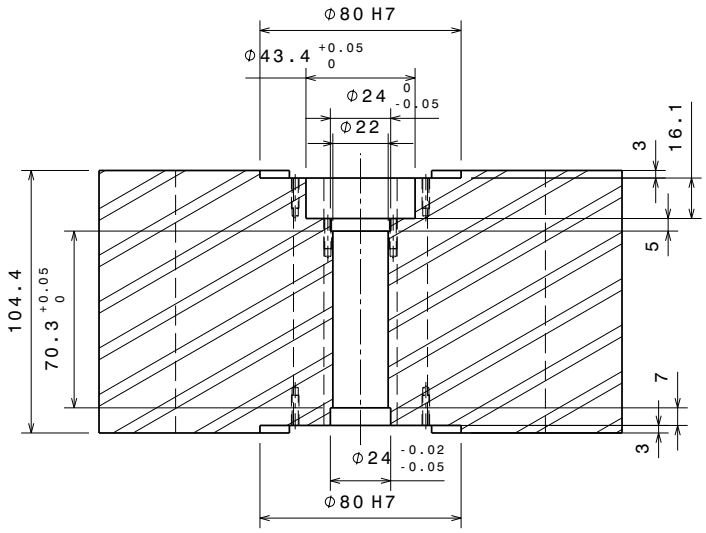

Coupe B-B
Echelle : 1:2

N°	Qté	PVC		2,2 Kg	
		Matière	Traitement de surface	Masse	Dessin d'ensemble
Rug. gén. : **Ra = 3,2**		Tol. gén. : **ISO 2768 mK**	Chanfreins: **0,2 à 45 °**	Projet :	**VIRGO**

CNRS - IN2P3
ULP
IPHC
Institut Pluridisciplinaire Hubert Curien STRASBOURG
23, rue du Loess - BP 28
67037 Strasbourg Cedex 02

ROTOR_S PVC

Dessiné par :	Vérifié par :	A3	Numéro	Echelle 1:2
V ZETER	Eddy			
le 15/02/2024				Révision

Copyright IN2P3 / IReS

Mitutoyo

CERTIFICATE OF INSPECTION

APPLICANT: Name _____

Address _____

INSTRUMENT: (1 set of 87) Gauge Block Material: Steel
Code No.: 516-947-10 Manufacturer: Mitutoyo
Type: BM1-87-1/PD Basis of Test: ISO3650/DIN861/JIS B7506
Serial No.: 1004326
Grade: 1 (JIS)

DATE OF INSPECTION: 06th Aug. 2010

INSPECTION METHOD: The length of gauge block is determined by comparing it, using a gauge block comparator, with a reference gauge block of the same nominal length. Both gauge blocks were placed in a vertical position on the comparator with their left or unmarked measuring face down. For determining the deviation / variation of length, dc / dmax / dmin / v is measured at the center point and the four corner points about 1.5 mm from the face edges.

ENVIRONMENT: Air temperature (20 ± 1.0) ℃

RESULTS: The results apply to the reference temperature of 20℃ (ITS-90).
For correction of the thermal expansion, an expansion coefficient of the gauge block of (6.0±0.3)×1E-6/F [(10.8±0.5)×1E-6/K] is used.
The result of the calibration are presented on the next page.

Expanded Uncertainty: (0.06 + 0.5L / 1000) μm (L = Nominal length) L:mm
(For Central Deviation)
(k=2)

The uncertainty presented above is based on a standard uncertainty multiplied by a coverage factor of k=2, which provides a confidence level of approximately 95%. The standard uncertainty has been determined in accordance with EAL-R2.

TRACEABILITY: Traceable to NIST No.821/276375-08
(NIST=National Institute of Standard and Technology)

Traceable to PTB via No.4937 PTB 06
(PTB=Physikalisch-Technische Bundesanstalt)

Date 06th Aug. 2010

A.Matsuura

F-687(8) MITUTOYO Co. HEADQUARTERS:
Postal code: 213-0012
20-1 Sakado 1-chome, Takatsu-ku, Kawasaki-shi.Japan
Tel: 044(813)8201 Fax: 044(813)8210

Result: The following table states for each gauge block the measured deviation from the nominal length at the center point and the measured deviation / variation of length.

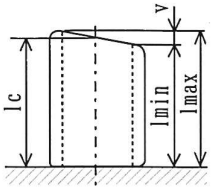

Nominal Length	ln	Maximum Deviation	dmax=lmax-ln
Central Length	lc	Minimum Length	lmin
Central Deviation	dc=lc-ln	Minimum Deviation	dmin=lmin-ln
Maximum Length	lmax	Variation	v=lmax-lmin

Unit: μm

Nominal Length mm ln	Ident. No.	Central Dev. dc	Max. Dev. dmax	Min. Dev. dmin	Var. v
0.5	100875	+0.01	+0.05	-0.03	0.08
1	100888	-0.08	-0.08	-0.11	0.03
1.001	100090	-0.02	-0.02	-0.03	0.01
1.002	100070	-0.03	-0.02	-0.04	0.02
1.003	100893	+0.03	+0.05	+0.02	0.03
1.004	100891	0.00	+0.01	-0.01	0.02
1.005	100422	+0.04	+0.05	-0.01	0.06
1.006	100596	-0.01	-0.01	-0.03	0.02
1.007	100286	-0.01	0.00	-0.02	0.02
1.008	100507	-0.02	0.00	-0.05	0.05
1.009	100321	0.00	+0.01	-0.01	0.02
1.01	100951	-0.01	+0.01	-0.01	0.02
1.02	100738	+0.03	+0.06	+0.03	0.03
1.03	100546	0.00	0.00	-0.02	0.02
1.04	100798	+0.04	+0.06	+0.01	0.05
1.05	100682	+0.03	+0.06	+0.01	0.05
1.06	100631	+0.05	+0.05	+0.04	0.01
1.07	100717	+0.02	+0.05	0.00	0.05
1.08	100840	+0.01	+0.04	-0.02	0.06
1.09	100273	0.00	+0.02	-0.02	0.04
1.1	100921	+0.01	+0.04	-0.01	0.05
1.11	100419	-0.02	+0.01	-0.03	0.04
1.12	100834	0.00	+0.02	-0.03	0.05
1.13	100101	-0.01	0.00	-0.07	0.07
1.14	100636	-0.04	-0.03	-0.06	0.03
1.15	100322	-0.06	-0.04	-0.08	0.04
1.16	100804	+0.01	+0.05	-0.01	0.06
1.17	100919	+0.01	+0.01	-0.01	0.02
1.18	100141	+0.02	+0.03	0.00	0.03
1.19	100244	-0.04	0.00	-0.05	0.05
1.2	100876	+0.02	+0.03	+0.01	0.02
1.21	100386	-0.02	0.00	-0.04	0.04
1.22	100868	-0.03	0.00	-0.03	0.03
1.23	100263	+0.02	+0.06	-0.01	0.07
1.24	100400	-0.03	0.00	-0.04	0.04
1.25	100831	-0.02	0.00	-0.03	0.03
1.26	100050	+0.01	+0.03	-0.01	0.04
1.27	100411	+0.02	+0.05	0.00	0.05
1.28	100964	-0.07	-0.06	-0.08	0.02

Unit: μm

Nominal Length mm ln	Ident. No.	Central Dev. dc	Max. Dev. dmax	Min. Dev. dmin	Var. v
1.29	100027	+0.02	+0.03	+0.02	0.01
1.3	080472	−0.05	−0.03	−0.06	0.03
1.31	100765	+0.02	+0.03	0.00	0.03
1.32	100157	0.00	0.00	−0.03	0.03
1.33	100432	+0.01	+0.02	0.00	0.02
1.34	100710	+0.01	+0.03	−0.02	0.05
1.35	100415	−0.02	+0.01	−0.04	0.05
1.36	100029	−0.02	+0.03	−0.03	0.06
1.37	100301	−0.03	−0.01	−0.04	0.03
1.38	100400	−0.03	−0.01	−0.04	0.03
1.39	100980	−0.02	0.00	−0.02	0.02
1.4	100879	−0.03	+0.02	−0.06	0.08
1.41	100919	−0.03	−0.01	−0.03	0.02
1.42	100300	−0.05	−0.02	−0.06	0.04
1.43	100462	0.00	+0.01	−0.06	0.07
1.44	100503	−0.10	−0.06	−0.14	0.08
1.45	100061	+0.02	+0.02	0.00	0.02
1.46	080204	−0.02	−0.02	−0.03	0.01
1.47	100029	−0.04	+0.01	−0.05	0.06
1.48	100594	−0.01	+0.01	−0.02	0.03
1.49	100323	−0.03	−0.02	−0.04	0.02
1.5	100093	−0.01	+0.01	−0.03	0.04
2	100756	+0.06	+0.06	+0.03	0.03
2.5	100621	−0.01	0.00	−0.01	0.01
3	100390	−0.01	0.00	−0.02	0.02
3.5	100763	0.00	+0.01	−0.01	0.02
4	100428	−0.02	−0.01	−0.03	0.02
4.5	100061	−0.06	−0.01	−0.08	0.07
5	100932	−0.05	−0.03	−0.09	0.06
5.5	100273	−0.02	+0.01	−0.05	0.06
6	101647	−0.06	−0.04	−0.07	0.03
6.5	100170	+0.01	+0.03	+0.01	0.02
7	101224	−0.02	+0.01	−0.02	0.03
7.5	100549	−0.02	+0.01	−0.02	0.03
8	101397	+0.02	+0.04	+0.02	0.02
8.5	100638	+0.03	+0.05	+0.01	0.04
9	101487	−0.06	−0.05	−0.09	0.04
9.5	100608	−0.03	+0.02	−0.03	0.05
10	102994	0.00	0.00	−0.07	0.07
20	101922	+0.01	+0.01	−0.02	0.03
30	101269	+0.13	+0.16	+0.08	0.08
40	100741	+0.03	+0.04	0.00	0.04
50	101173	+0.09	+0.12	+0.06	0.06
60	100449	+0.08	+0.11	+0.08	0.03
70	090274	+0.15	+0.16	+0.15	0.01

Mitutoyo Cales Etalon

Unit: μm

Nominal Length mm ln	Ident. No.	Central Dev. dc	Max. Dev. dmax	Min. Dev. dmin	Var. v
80	100216	+0.08	+0.16	+0.07	0.09
90	090906	+0.05	+0.05	-0.12	0.17
100	100566	+0.13	+0.13	+0.06	0.07